SCIENTIFIC REPORTS

OPEN

Dynamic generation of multi-qubit entanglement in the ultrastrong-coupling regime

Received: 28 August 2018
Accepted: 16 January 2019
Published online: 27 February 2019

Xin Liu[1], Qinghong Liao[2], Guangyu Fang[3] & Shutian Liu[3]

We propose a dynamic evolution protocol for generating multi-qubit GHZ states in the ultrastrong-coupling regime of circuit QED. By varying the time length of sequences, the protocol works for any coupling strength $g/\omega_r \geq 0.25$. The time for generating the GHZ states in our protocol can be in the subnanoseconds. By taking into account realistic parameters of circuit QED, the degeneracy of fidelity due to decoherence can be as low as 0.02%.

The realization of a controllable platform consisting of two-level systems interacting with a discrete electromagnetic field has been a milestone in the history of quantum physics. Nowadays, the well-known cavity quantum electrodynamics has been greatly studied in the past decades and a lot of applications in quantum information processing have been proposed[1–14]. As usual, all these studies were concentrated on the weak or strong coupling regime where the coupling strength between the two-level system and the cavity mode is much smaller than the frequency of the cavity mode. In recent years, the so-called ultrastrong-coupling regime of a two-level system interacting with a cavity mode was realized experimentally[15–17], where the coupling strength is comparable to the frequency of the cavity mode, facilitating a concrete realization of the quantum Rabi model. Furthermore, even a deep strong coupling regime where the coupling strength is larger than the frequency of the cavity mode was realized[18]. In this new light-matter interacting regime, a lot of novel phenomena and processes emerged, as conservation of the eigenstate parity[19], degeneracy of vacuum[20], absence of Berry phase[21], non-classical radiation from the thermal cavities[22], and many efforts were devoted to these phenomena[23–36]. These findings enriched the contents of cavity QED theory, but ideas of how to control and exploit these processes in quantum information processing are still limited[37–42]. In 2012, Romero *et al.* proposed an architecture and a scheme to realize ultrafast logical gates based on the quantum Rabi model[37]. Wu *et al.* proposed to generate Dicke states utilizing selective resonant interactions in the ultrastrong-coupling regime, but the state fidelities were limited[38]. A protocol for harvesting the entanglement of the ground states manifold in the deep strong coupling regime was designed based on the adiabatic processes[39]. However, applications of the ultrastrong-coupling regime are still on the early stage compared with vast schemes in the literature lying in the weak or strong coupling regime.

On the other hand, entanglement plays an important role both in the principles of quantum mechanics and in the implementations of quantum information processing[43,44]. Two-qubit or multi-qubit entanglement is an essential resource in the quantum information tasks. Many efforts have been devoted to the protocols for generating multi-qubit entanglement[5,11–13,45–50]. Unfortunately, due to the fragile nature of quantum entanglement, generation of multi-qubit entanglement has always been a challenging issue. As an expected situation, there are few schemes for generating multi-qubit entanglement in this new ultrastrong-coupling regime and potential applications need to be exploited.

In this paper, we propose a dynamic evolution protocol for generation of GHZ states in the ultrastrong-coupling regime of circuit QED. The scheme works for any coupling strength $g/\omega_r \geq 0.25$. Using a sequence of different time length pulses in different coupling strengths, the multi-qubit entanglement can be generated in subnanoseconds. The advance of this scheme is the quite low decoherence influence due to the special decay processes in the ultrastrong-coupling regime. The influence of inhomogeneous parameters is also discussed, which shows fidelities above 99% of the aimed states under imperfect parameters.

[1]School of Physics and Technology, University of Jinan, Jinan, 250022, People's Republic of China. [2]Department of Electronic Information Engineering, Nanchang University, Nanchang, 330031, People's Republic of China. [3]Department of Physics, Harbin Institute of Technology, Harbin, 150001, People's Republic of China. Correspondence and requests for materials should be addressed to X.L. (email: sps_liux@ujn.edu.cn)

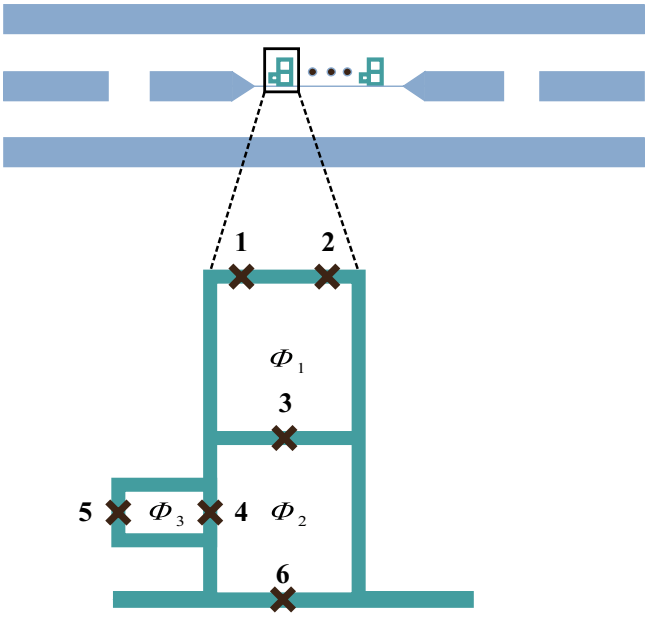

Figure 1. Schematic diagram of the system consisting of six-junction flux qubits galvanically coupled to a transmission-line resonator. The black crosses denote the Josephson junctions and Φ_1, Φ_2 and Φ_3 are external tunable fluxes.

The Model and Protocol

The architecture we consider is schematically illustrated in Fig. 1, where multiple six-junction superconducting flux qubits are galvanically coupled to a coplanar wave-guide resonator. In this qubit design, the longitudinal and transversal coupling of qubits with resonator mode could be tuned by the flux Φ_1 in the qubit loop[37] and more coupled qubits could be added by prolonging the length of resonator. By adjusting the coupling with only the longitudinal component and assuming a uniform coupling strength for all the qubits (fluctuation of the coupling strength will be considered later), we obtain the system Hamiltonian to be

$$H = \omega_r a^\dagger a + \sum_i \frac{\omega_q}{2}\sigma_x^i + \sum_i g(a + a^\dagger)\sigma_x^i \tag{1}$$

where ω_r represents the frequency of resonator mode, ω_q is the frequency of a six-junction qubit, and g is the coupling strength between the qubits and the resonator mode. The coupling strength g can be adjusted by the flux Φ_3 in the additional loop of a qubit, and each qubit and the flux in each loop of the qubit can be addressed and tuned individually[37].

In the interaction picture, the Hamiltonian in Eq. (1) takes a form

$$H_I = g(ae^{-i\omega_r t} + a^\dagger e^{i\omega_r t})S_x \tag{2}$$

with $S_x = \sum_i \sigma_x^i$. The time evolution operator corresponding to the Hamiltonian in Eq. (2) can be written in a factorized way as[7,47,51]

$$U_I(t) = e^{-iA(t)S_x^2} e^{-iF(t)S_x a} e^{-iG(t)S_x a^\dagger} \tag{3}$$

By substituting the expression of time evolution operator in Eq. (3) into the equation $i[\partial/\partial t U_I(t)]U_I^{-1}(t) = H_I(t)$, the coefficients in Eq. (3) can be obtained as

$$A(t) = -\frac{g^2}{\omega_r}\left[t - \frac{1}{i\omega_r}(e^{i\omega_r t} - 1)\right] \tag{4}$$

$$F(t) = \frac{ig}{\omega_r}(e^{-i\omega_r t} - 1) \tag{5}$$

$$G(t) = \frac{g}{i\omega_r}(e^{i\omega_r t} - 1) \tag{6}$$

Therefore, the time evolution operator in the Schrödinger picture is

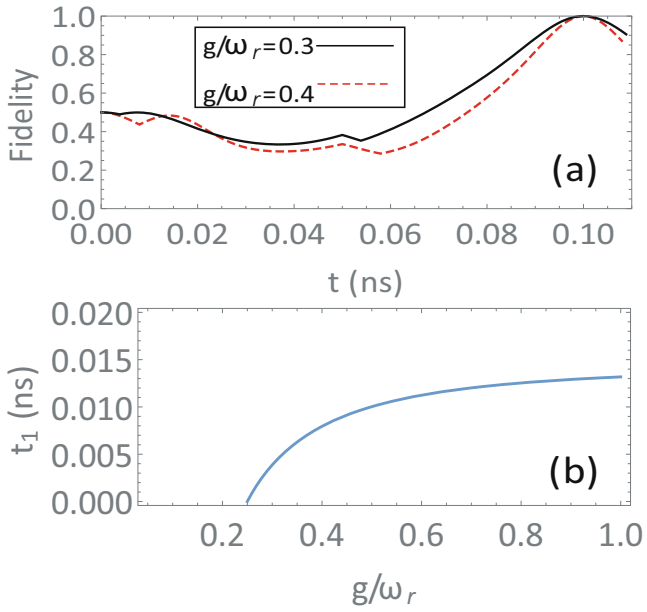

Figure 2. (**a**) The time evolution of the fidelities of the qubits states and the GHZ state for different coupling strengths $g/\omega_r = 0.3$ (black solid line) and $g/\omega_r = 0.4$ (red dashed line). The unity fidelity is reached at $t = 0.1$ ns under unitary evolution for the four-step protocol. (**b**) The needed time of the first step t_1 under different coupling strengths (scaled by the resonator frequency ω_r). By varying the time of the first step t_1, the protocol works for any coupling strength $g/\omega_r \geq 0.25$.

$$U(t) = e^{-i\omega_r t a^\dagger a} e^{-i\omega_q t S_x/2} e^{-iA(t)S_x^2} e^{-iF(t)S_x a} e^{-iG(t)S_x a^\dagger} \tag{7}$$

In the following, we will mainly use the time evolution operator in Eq. (7) to construct an evolution to GHZ states.

Our protocol for generating GHZ states is implemented in the following four steps. First, tune the coupling strength between the qubits and the resonator to a value g and evolve for a time interval $\omega_r t_1 \in [0, \pi]$. The second step, tune the coupling strength between the qubits and the resonator to a negative value $-g$ and evolve for another period $\omega_r t_2 = \pi - \omega_r t_1$. The third step, repeat the step 1 and the fourth step, repeat the step 2.

The total time evolution operator of four steps is written as (see Methods for detailed calculation)

$$U = U_4(t_2)U_3(t_1)U_2(t_2)U_1(t_1) = e^{\left[2i\pi\frac{g^2}{\omega_r^2} - 8i\frac{g^2}{\omega_r^2}\sin(\omega_r t_1)\right]S_x^2} \tag{8}$$

In the total time evolution operator in Eq. (8), the evolutions of the qubits and the resonator are separated and a qubit-qubit XX type interaction is generated despite of individual qubit rotation. This XX type interaction is suitable for the gate for GHZ states[5], if we set the phase to satisfy

$$2\pi\frac{g^2}{\omega_r^2} - 8\frac{g^2}{\omega_r^2}\sin(\omega_r t_1) = (1 + 4m)\frac{\pi}{8} \tag{9}$$

with m being an arbitrary integer.

With this phase in rotation in Eq. (8), stating from the qubits state $\otimes_{i=1}^N |-\rangle^i$ with an even number of qubits N, where $|-\rangle^i$ and $|+\rangle^i$ are the eigenstates of the σ_z^i operator of every qubit $\sigma_z^i|-\rangle^i = -|-\rangle^i$, $\sigma_z^i|+\rangle^i = |+\rangle^i$, a GHZ state $\frac{1}{\sqrt{2}}(\otimes_{i=1}^N |-\rangle^i + e^{i\pi(N+1)/2} \otimes_{i=1}^N |+\rangle^i)$ is obtained in any qubit-resonator coupling strength $g/\omega_r \geq 0.25$ in the ultrastrong-coupling regime. For an odd number of qubits, an additional single-qubit rotation $\exp(-\pi S_x/4)$ is needed despite of the phase in Eq. (9), and the obtained GHZ state is $\frac{1}{\sqrt{2}}(\otimes_{i=1}^N |-\rangle^i + e^{i\pi N/2} \otimes_{i=1}^N |+\rangle^i)$.

Results

In this section, we simulate the scheme presented above in a four-qubit case. In a four-qubit case, the initial state is $|-\rangle^1|-\rangle^2|-\rangle^3|-\rangle^4$. This state can be realized by biasing the qubits far away from the degeneracy point with the coupling between the qubits and the resonator shut down, relaxing the qubits to their ground states, and then biasing them back non-adiabatically and applying a $\pi/2$ pulse for all the qubits.

By setting the initial resonator state in the vacuum state $|0\rangle$, the evolution of fidelity of the qubits state and the GHZ state is presented in Fig. 2(a) for coupling strengths $g/\omega_r = 0.3$ and $g/\omega_r = 0.4$. The frequency of the first mode of a transmission line resonator could be $1 \times 2\pi \sim 10 \times 2\pi$ GHz. In the simulation, a frequency of $10 \times 2\pi$ GHz is chosen. It could be seen that in $t = 2\pi/\omega_r = 0.1$ ns exact GHZ states are obtained for any coupling strength.

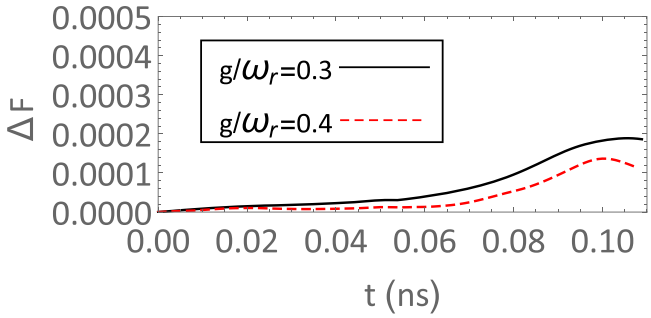

Figure 3. The evolution of fidelity deviations ($\Delta F = F - F_d$ with F being the fidelity under the unitary evolution and F_d being the fidelity with decay) with time for different coupling strengths $g/\omega_r = 0.3$ (black solid line) and $g/\omega_r = 0.4$ (red dashed line). The other parameters are $\omega_r = 10 \times 2\pi$ GHz, $Q = 2 \times 10^5$, $T_1 = 1.5\,\mu$s.

In Fig. 2(b), the evolution time of the first step is presented according to Eq. (9). It could be seen that the evolution time t_1 needed grows slightly with the increase of qubit-resonator coupling strength, and evolutions to GHZ states in different coupling strengths could be realized by adjusting the evolution time t_1.

In the last paragraph, we simulate our protocol with a unitary evolution, and a unity fidelity can be obtained. However, the advance of the protocol will be prominent only when one takes into account the decay of the procedure. In the ultrastrong-coupling regime, the standard master equation fails to describe the decoherence of system because it predicts some unphysical results. A proper way is to expand the system-bath interaction Hamiltonian in the basis of system Hamiltonian eigenstates and after applying the standard Markov approximation and tracing out the reservoirs degrees of freedom, a master equation describing the decoherence of quantum Rabi model can be obtained as[22,52]

$$\dot{\rho}(t) = i[\rho(t), H] + \sum_{\lambda}\sum_{j,k>j}\Gamma_{\lambda}^{jk} D[|j\rangle\langle k|]\rho(t) \tag{10}$$

where $|j\rangle$ is the j-th eigenstate of the system Hamiltonian with the eigenstates labeled by the corresponding eigenvalues in an increasing order and the super-operator $D[O]\rho$ takes the form $D[O]\rho = \frac{1}{2}(2O\rho O^{\dagger} - \rho O^{\dagger}O - O^{\dagger}O\rho)$. The subscript λ represent the decay from the cavity (λ_c) and the decay from the qubits (λ_1, λ_2, λ_3, λ_4). The relaxation coefficients can take a simplified form $\Gamma_{\lambda}^{jk} = \gamma_{\lambda}\left|C_{j,k}^{(\lambda)}\right|^2$ with γ_{λ} being the standard damping rates in a weak coupling scenario and $C_{jk}^{(\lambda)} = \langle j|(c_{\lambda} + c_{\lambda}^{\dagger})|k\rangle$, after assuming constant spectral densities and constant system-bath coupling strengths.

In the simulation, a qubit relaxation time $T_1 = 1.5\,\mu$s and a cavity quality factor $Q = 2 \times 10^5$ are assumed, which has been realized in a flux qubit experiment[53] and is not very high for a transmission line resonator[54]. In Fig. 3, fidelity deviations ΔF between the unitary evolutions and the evolutions with the cavity and qubits decay are plotted. It is shown that the deviations grow as time passes and fidelity deviations under 0.02% can be obtained at $t = 0.1$ ns, which is greatly suppressed compared with some schemes working in the strong coupling regime[12,46,50]. In the above master equation, dephasing effect was not included in calculation. However, by considering a dephasing time of more than 1 μs in ref.[55], we can still hope a state fidelity up to 99%. Or in an alternative way, like the method done in ref.[18], tuning the flux qubit in the degeneracy point, and setting the frequency of resonator much larger than the qubit gap Δ will also consist the model of Eq. (2) used in our scheme, while dephasing effect will be largely suppressed.

For a realistic experimental implementation of circuit QED system, the fluctuations of parameters of qubits and qubit-resonator coupling strengths are unavoidable. We simulate the influence of fluctuations of these parameters on the fidelities of aimed states in Fig. 4. We evaluate mean fidelities and standard deviations of the maximal fidelities in a few single evolution procedures with random values of a parameter. We show the influence of these fluctuations of parameters with fluctuation of one parameter in one figure. For one parameter, we assumed a random value for each of the qubit in Gaussian distribution with a standard deviation δr. For each deviation, 100 times single evolution of the protocol is calculated and the mean value and deviation of the maximal fidelities are calculated. The influences of random $\delta\varepsilon$, $\delta\omega_q$ and δg (corresponding to the strengths of the σ_z, σ_x components of the qubits and the coupling strength of the qubits and the resonator, respectively) are shown in Fig. 4(a–c) respectively, which rise from fluctuations of the magnetic flux and fabrication imperfections. It is shown that the mean fidelities decrease and the corresponding standard deviations increase as growing of the fluctuations of parameters, as expected. Under the fluctuations of parameters with standard deviation 2.5%, the fidelities of protocol still keep up to 99% and the fluctuation of coupling strength g changes the fidelity more dramatically.

Discussion

In practical implementation of our scheme in circuit QED, the most challenging problem may be the control pulses with high switching frequency and well-defined shape. Indeed, high switching frequency pulses up to 10 GHz have already been realized in experiment[56]. We can expect pulses with higher frequency will be realized in state-of-the-art circuit QED experiments. Besides, with the same parameters in Fig. 2a, we simulated the fidelity evolution with coupling strength g in a smooth error function profile as what were did in refs[57,58] with a standard deviation 0.005 ns of Gaussian and a maximal fidelity above 99.1% can be obtained. The coplanar transmission line resonator is a

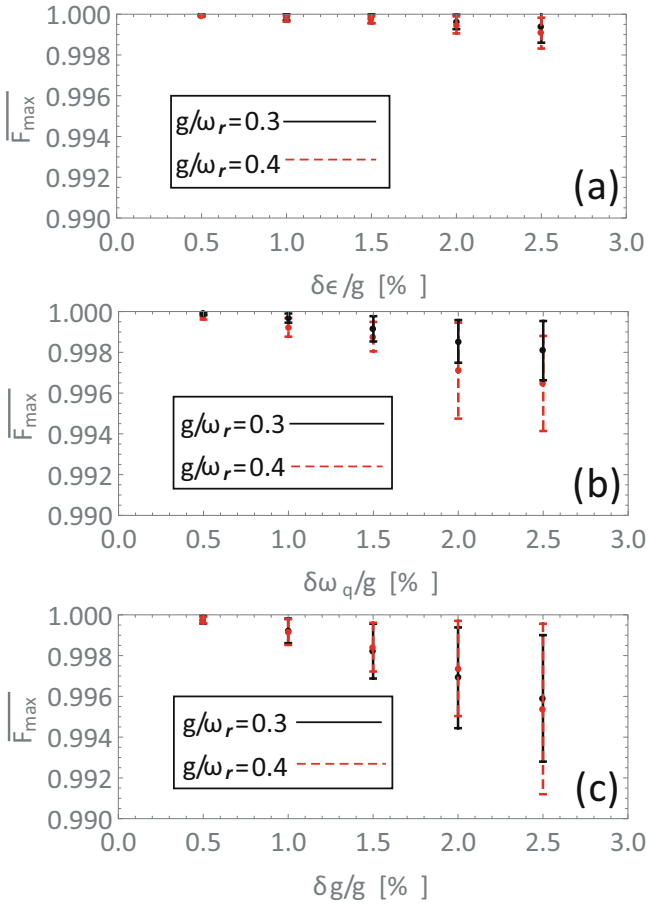

Figure 4. The influences on the fidelities caused by inhomogeneous (**a**) ε, (**b**) ω_q and (**c**) g (corresponding to the strengths of the σ_z, σ_x components of the qubits and the coupling strength of the qubits and the resonator) individually. The longitudinal axes show the mean fidelities and the standard deviations of the fidelities for a fixed deviation of the parameter (scaled by the coupling strength g). The parameters are $\omega_r = 10 \times 2\pi$ GHz, $g/\omega_r = 0.3$ (black solid line) and $g/\omega_r = 0.4$ (red dashed line) and the number of the random evolutions is $n_r = 100$.

one-dimension cavity with multiple modes. Without the rotating-wave approximation, higher modes will have influential couplings with the qubits. Based on the multi-mode quantum Rabi model, the higher modes don't change the form of time evolution operator in Eq. (7), so they won't change the fidelity of the protocol. The only effect is the summary of multiple modes in the exponential component in Eq. (7) will modify the phases in Eq. (18), resulting in a new phase equation which time t_1 should satisfy $\sum_{\tilde{n}=1}^{n_c} 2\pi(g_{\tilde{n}}^2/\omega_{\tilde{n}}^2) - 8(g_{\tilde{n}}^2/\omega_{\tilde{n}}^2)\sin(\omega_{\tilde{n}} t_1) = \pi/8$, where the $g_{\tilde{n}}$ and $\omega_{\tilde{n}}$ are coupling strength and mode frequency of mode $\tilde{n}$ and n_c is the cutoff number of cavity modes. With this time length of t_1 satisfying new phase equation, the protocol could be implemented with unity fidelity. It will be noticed that there already exist some schemes for generating multi-qubit entanglement in the ultrastrong-coupling regime[29,38,39,47,59,60], which may have some similarities with the protocol here, especially the scheme in ref.[47]. However, we clarify the protocol here is exactly an extension of scheme in ref.[47]. In Fig. 2b, it will be find our protocol reduce to the protocol in ref.[47] at $g/\omega_r = 0.25$, where the time t_1 reduces to zero and the one-step protocol in ref.[47] is recovered. On the other hand, compared with the protocol in ref.[47] working for some special coupling strengths fixed by two integers, our protocol works for any coupling strength by varying the time length of first step, releasing a parameter constriction.

In summary, we propose a dynamic scheme for generating multi-qubit GHZ states in the ultrastrong-coupling regime. The scheme can generate the GHZ states with unity fidelity in subnanoseconds under unitary evolution. More astonishingly, the deviation caused by the decay of the qubits and resonator is greatly suppressed to below 0.02%. The scheme works for any qubit-resonator coupling strength $g/\omega_r \geq 0.25$ and the operation time does not change with the increasing of the qubit number. The influences of inhomogeneous parameters are also discussed. We hope the scheme can provide a realizable method for generating multi-qubit entanglement in the ultrastrong-coupling regime of cavity QED.

Methods

The time evolution operator in Eq. (7) corresponding to step one and step three can be rewritten as

$$\begin{aligned} U_{1,3} &= e^{-i\omega_r t a^\dagger a} e^{-i\omega_q t S_x/2} e^{-iA(t)S_x^2} e^{-\frac{1}{2}|F(t)|^2 S_x^2} e^{[-iF(t)S_x a - iF^*(t)S_x a^\dagger]} \\ &= e^{-i\omega_r t a^\dagger a} e^{-i\omega_q t S_x/2} e^{\left[-iA(t)-\frac{1}{2}|F(t)|^2\right]S_x^2} \mathrm{D}(-iF^*(t)S_x) \end{aligned} \tag{11}$$

with $\mathrm{D}(\beta S_x) = \exp[(\beta a^\dagger - \beta^* a)S_x]$ being the controlled coherent displacement of the field. In step two and step four, the system Hamiltonian in the interaction picture can be written as

$$H_I = -g(ae^{-i\omega_r t} + a^\dagger e^{i\omega_r t})S_x \tag{12}$$

The corresponding time evolution operator in the Schrödinger picture is

$$U(t) = e^{-i\omega_r t a^\dagger a} e^{-i\omega_q t S_x/2} e^{-iA'(t)S_x^2} e^{-iG'(t)S_x a^\dagger} e^{-iF'(t)S_x a} \tag{13}$$

with

$$A'(t) = \left(\frac{g^2}{\omega_r}\right)\left[\frac{1}{-i\omega_r}(e^{-i\omega_r t} - 1) - t\right] \tag{14}$$

$$G'(t) = -\frac{g}{i\omega_r}(e^{i\omega_r t} - 1) \tag{15}$$

$$F'(t) = \frac{g}{i\omega_r}(e^{-i\omega_r t} - 1) \tag{16}$$

The time evolution operator corresponding to step two and step four can be rewritten as

$$\begin{aligned} U_{2,4} &= e^{-i\omega_r t a^\dagger a} e^{-i\omega_q t S_x/2} e^{-iA'(t)S_x^2} e^{\frac{1}{2}|F'(t)|^2 S_x^2} e^{[-iF'^*(t)S_x a^\dagger - iF(t)S_x a]} \\ &= e^{-i\omega_r t a^\dagger a} e^{-i\omega_q t S_x/2} e^{\left[-iA'(t)+\frac{1}{2}|F'(t)|^2\right]S_x^2} \mathrm{D}(-iF'^*(t)S_x) \end{aligned} \tag{17}$$

The total time evolution operator of the four steps will be

$$\begin{aligned} U &= U_4(t_2)U_3(t_1)U_2(t_2)U_1(t_1) \\ &= e^{-i\omega_r t_2 a^\dagger a} e^{[-iA'(t_2)+\frac{1}{2}|F'(t_2)|^2]S_x^2} \mathrm{D}(-iF'^*(t_2)S_x) e^{-i\omega_r t_1 a^\dagger a} e^{[-iA(t_1)-\frac{1}{2}|F(t_1)|^2]S_x^2} \mathrm{D}(-iF^*(t_1)S_x) \\ &\quad e^{-i\omega_r t_2 a^\dagger a} e^{[-iA'(t_2)+\frac{1}{2}|F'(t_2)|^2]S_x^2} \mathrm{D}(-iF'^*(t_2)S_x) e^{-i\omega_r t_1 a^\dagger a} e^{[-iA(t_1)-\frac{1}{2}|F(t_1)|^2]S_x^2} \mathrm{D}(-iF^*(t_1)S_x) \\ &= e^{-i\pi a^\dagger a} e^{[-iA'(t_2)+\frac{1}{2}|F'(t_2)|^2]S_x^2} \mathrm{D}(-iF'^*(t_2)e^{i\omega_r t_1}S_x) e^{[-iA(t_1)-\frac{1}{2}|F(t_1)|^2]S_x^2} \mathrm{D}(-iF^*(t_1)S_x) \\ &\quad e^{-i\pi a^\dagger a} e^{[-iA't_2)+\frac{1}{2}|F'(t_2)|^2]S_x^2} \mathrm{D}(-iF'^*(t_2)e^{i\omega_r t_1}S_x) e^{[-iA(t_1)-\frac{1}{2}|F(t_1)|^2]S_x^2} \mathrm{D}(-iF^*(t_1)S_x) \\ &= e^{[-2iA'(t_2)+|F'(t_2)|^2-2iA(t_1)-|F(t_1)|^2]S_x^2} e^{i\mathrm{Im}[-iF'^*(t_2)e^{i\omega_r t_1} iF(t_1)S_x^2]} \\ &\quad \mathrm{D}[(-iF'^*(t_2)e^{i\omega_r t_1} - iF^*(t_1))e^{-i\pi}S_x] \\ &\quad e^{i\mathrm{Im}[-iF'^*(t_2)e^{i\omega_r t_1} iF(t_1)S_x^2]} \mathrm{D}[(-iF'^*(t_2)e^{i\omega_r t_1} - iF^*(t_1))S_x] \\ &= e^{[-2iA'(t_2)+|F'(t_2)|^2-2iA(t_1)-|F(t_1)|^2]S_x^2} e^{i2\mathrm{Im}[-iF'^*(t_2)e^{i\omega_r t_1} iF(t_1)S_x^2]} \\ &\quad e^{i\mathrm{Im}[(-iF'^*(t_2)e^{i\omega_r t_1} - iF^*(t_1))e^{-i\pi}(iF'(t_2)e^{-i\omega_r t_1} + iF(t_1))S_x^2]} \\ &= \exp\left\{\left[2i\pi\frac{g^2}{\omega_r^2} - 4i\frac{g^2}{\omega_r^2}\sin(\omega_r t_1)\right]S_x^2\right\} \exp\left\{\left[-4i\frac{g^2}{\omega_r^2}\sin(\omega_r t_1)\right]S_x^2\right\} \\ &= e^{[2i\pi\frac{g^2}{\omega_r^2} - 8i\frac{g^2}{\omega_r^2}\sin(\omega_r t_1)]S_x^2} \end{aligned} \tag{18}$$

where we have omitted rotation rising from S_x component which just generates trivial single qubit rotation. In the calculation, equations $\mathrm{D}(\alpha)\mathrm{D}(\beta) = e^{i\mathrm{Im}(\alpha\beta^*)}\mathrm{D}(\alpha+\beta)$ and $e^{-i\theta a^\dagger a}\mathrm{D}(\alpha)e^{i\theta a^\dagger a} = \mathrm{D}(\alpha e^{-i\theta})$ are used.

References

1. Devoret, M. H. & Schoelkopf, R. J. Superconducting circuits for quantum information: an outlook. *Science* **339**, 1169 (2013).
2. Monroe, C. & Kim, J. Scaling the ion trap quantum processor. *Science* **339**, 1164 (2013).
3. Wendin, G. Quantum information processing with superconducting circuits: a review. *Rep. Prog. Phys.* **80**, 106001 (2017).
4. Gu, X., Kockum, A. F., Miranowicz, A., Liu, Y. X. & Nori, F. Microwave photonics with superconducting quantum circuits. *Physics Reports* **718–719**, 1 (2017).
5. Mølmer, K. & Sørensen, A. Multiparticle entanglement of hot trapped ions. *Phys. Rev. Lett.* **82**, 1835 (1999).
6. Sørensen, A. & Mølmer, K. Quantum computation with ions in thermal motion. *Phys. Rev. Lett.* **82**, 1971 (1999).
7. Sørensen, A. & Mølmer, K. Entanglement and quantum computation with ions in thermal motion. *Phys. Rev. A* **62**, 022311 (2000).
8. Blatt, R. & Wineland, D. Entangled states of trapped atomic ions. *Nature* **453**, 1008 (2008).
9. Marr, C., Beige, A. & Rempe, G. Entangled-state preparation via dissipation-assisted adiabatic passages. *Phys. Rev. A* **68**, 033817 (2003).

10. Chen, C. Y., Feng, M. & Gao, K. L. Toffoli gate originating from a single resonant interaction with cavity QED. *Phys. Rev. A* **73**, 064304 (2006).
11. Gonţa, D., Fritzsche, S. & Radtke, T. Generation of four-partite Greenberger-Horne-Zeilinger and W states by using a high-finesse bimodal cavity. *Phys. Rev. A* **77**, 062312 (2008).
12. Bishop, L. S. *et al*. Proposal for generating and detecting multi-qubit GHZ states in circuit QED. *New J. Phys.* **11**, 073040 (2009).
13. Peng, Z. H., Liu, Y. X., Nakamura, Y. & Tsai, J. S. Fast generation of multiparticle entangled state for flux qubits in a circle array of transmission line resonators with tunable coupling. *Phys. Rev. B* **85**, 024537 (2012).
14. Zheng, S. B., Yang, Z. B. & Xia, Y. Generation of two-mode squeezed states for two separated atomic ensembles via coupled cavities. *Phys. Rev. A* **81**, 015804 (2010).
15. Niemczyk, T. *et al*. Circuit quantum electrodynamics in the ultrastrong-coupling regime. *Nat. Phys.* **6**, 772 (2010).
16. Forn-Díaz, P. *et al*. Observation of the Bloch-Siegert shift in a qubit-oscillator system in the ultrastrong coupling regime. *Phys. Rev. Lett.* **105**, 237001 (2010).
17. Schwartz, T., Hutchison, J. A., Genet, C. & Ebbesen, T. W. Reversible switching of ultrastrong light-molecule coupling. *Phys. Rev. Lett.* **106**, 196405 (2011).
18. Yoshihara, F. *et al*. Superconducting qubit–oscillator circuit beyond the ultrastrong-coupling regime. *Nat. Phys.* **13**, 44 (2017).
19. Casanova, J., Romero, G., Lizuain, I., García-Ripoll, J. J. & Solano, E. Deep strong coupling regime of the Jaynes-Cummings model. *Phys. Rev. Lett.* **105**, 263603 (2010).
20. Nataf, P. & Ciuti, C. Vacuum degeneracy of a circuit QED system in the ultrastrong coupling regime. *Phys. Rev. Lett.* **104**, 023601 (2010).
21. Larson, J. Absence of vacuum induced Berry phases without the rotating wave approximation in cavity QED. *Phys. Rev. Lett.* **108**, 033601 (2012).
22. Ridolfo, A., Savasta, S. & Hartmann, M. J. Nonclassical radiation from thermal cavities in the ultrastrong coupling regime. *Phys. Rev. Lett.* **110**, 163601 (2013).
23. Hausinger, J. & Grifoni, M. Qubit-oscillator system: An analytical treatment of the ultrastrong coupling regime. *Phys. Rev. A* **82**, 062320 (2010).
24. Peropadre, B., Forn-Díaz, P., Solano, E. & García-Ripoll, J. J. Switchable ultrastrong coupling in circuit QED. *Phys. Rev. Lett.* **105**, 023601 (2010).
25. Zhang, Y. *et al*. Analytical ground state for the Jaynes-Cummings model with ultrastrong coupling. *Phys. Rev. A* **83**, 065802 (2011).
26. Lee, K. M. & Law, C. K. Ground state of a resonant two-qubit cavity system in the ultrastrong-coupling regime. *Phys. Rev. A* **88**, 015802 (2013).
27. Stassi, R., Ridolfo, A., Di Stefano, O., Hartmann, M. J. & Savasta, S. Spontaneous conversion from virtual to real photons in the ultrastrong-coupling regime. *Phys. Rev. Lett.* **110**, 243601 (2013).
28. Huang, J. F. & Law, C. K. Photon emission via vacuum-dressed intermediate states under ultrastrong coupling. *Phys. Rev. A* **89**, 033827 (2014).
29. Garziano, L. *et al*. Multiphoton quantum Rabi oscillations in ultrastrong cavity QED. *Phys. Rev. A* **92**, 063830 (2015).
30. Le Boité, A., Hwang, M. J., Nha, H. & Plenio, M. B. Fate of photon blockade in the deep strong-coupling regime. *Phys. Rev. A* **94**, 033827 (2016).
31. Garziano, L. *et al*. One photon can simultaneously excite two or more atoms. *Phys. Rev. Lett.* **117**, 043601 (2016).
32. Garziano, L., Ridolfo, A., De Liberato, S. & Savasta, S. Cavity QED in the ultrastrong coupling regime: photon bunching from the emission of individual dressed qubits. *ACS Photonics* **4**, 2345 (2017).
33. Langford, N. K. *et al*. Experimentally simulating the dynamics of quantum light and matter at deep-strong coupling. *Nat. Commun.* **8**, 1715 (2017).
34. Kockum, A. F., Miranowicz, A., Macrì, V., Savasta, S. & Nori, F. Deterministic quantum nonlinear optics with single atoms and virtual photons. *Phys. Rev. A* **95**, 063849 (2017).
35. Forn-Díaz, P., Lamata, L., Rico, E., Kono, J. & Solano, E. Ultrastrong coupling regimes of light-matter interaction. *arXiv* **1804**, 09275 (2018).
36. Kockum, A. F., Miranowicz, A., De Liberato, S., Savasta, S. & Nori, F. Ultrastrong coupling between light and matter. *Nature Reviews Physics* **1**, 19–40 (2019).
37. Romero, G., Ballester, D., Wang, Y. M., Scarani, V. & Solano, E. Ultrafast quantum gates in circuit QED. *Phys. Rev. Lett.* **108**, 120501 (2012).
38. Wu, C. *et al*. Generation of Dicke states in the ultrastrong-coupling regime of circuit QED systems. *Phys. Rev. A* **95**, 013845 (2017).
39. Armata, F., Calajo, G., Jaako, T., Kim, M. S. & Rabl, P. Harvesting multiqubit entanglement from ultrastrong interactions in circuit quantum electrodynamics. *Phys. Rev. Lett.* **119**, 183602 (2017).
40. Kyaw, T. H., Felicetti, S., Romero, G., Solano, E. & Kwek, L. C. Scalable quantum memory in the ultrastrong coupling regime. *Sci. Rep.* **5**, 8621 (2015).
41. Wang, Y., Zhang, J., Wu, C., You, J. Q. & Romero, G. Holonomic quantum computation in the ultrastrong-coupling regime of circuit QED. *Phys. Rev. A* **94**, 012328 (2016).
42. Wang, Y., Guo, C., Zhang, G. Q., Wang, G. & Wu, C. Ultrafast quantum computation in ultrastrongly coupled circuit QED systems. *Sci. Rep.* **7**, 44251 (2017).
43. Horodecki, R., Horodecki, P., Horodecki, M. & Horodecki, K. Quantum entanglement. *Rev. Mod. Phys.* **81**, 865 (2009).
44. Montanaro, A. Quantum algorithms: an overview. *npj Quantum Information* **2**, 15023 (2016).
45. Deng, Z. J., Feng, M. & Gao, K. L. Simple scheme for generating an n-qubit W state in cavity QED. *Phys. Rev. A* **73**, 014302 (2006).
46. Lin, X. M., Xue, P., Chen, M. Y., Chen, Z. H. & Li, X. H. Scalable preparation of multiple-particle entangled states via the cavity input-output process. *Phys. Rev. A* **74**, 052339 (2006).
47. Wang, Y. D., Chesi, S., Loss, D. & Bruder, C. One-step multiqubit Greenberger-Horne-Zeilinger state generation in a circuit QED system. *Phys. Rev. B* **81**, 104524 (2010).
48. Aldana, S., Wang, Y. D. & Bruder, C. Greenberger-Horne-Zeilinger generation protocol for N superconducting transmon qubits capacitively coupled to a quantum bus. *Phys. Rev. B* **84**, 134519 (2011).
49. Facchi, P., Florio, G., Pascazio, S. & Pepe, F. V. Greenberger-Horne-Zeilinger states and few-body Hamiltonians. *Phys. Rev. Lett.* **107**, 260502 (2011).
50. Yang, C. P., Su, Q. P., Zheng, S. B. & Nori, F. Entangling superconducting qubits in a multi-cavity system. *New J. Phys.* **18**, 013025 (2016).
51. Wei, J. & Norman, E. Lie algebraic solution of linear differential equations. *J. Math. Phys.* **4**, 575 (1963).
52. Beaudoin, F., Gambetta, J. M. & Blais, A. Dissipation and ultrastrong coupling in circuit QED. *Phys. Rev. A* **84**, 043832 (2011).
53. Fedorov, A. *et al*. Strong coupling of a quantum oscillator to a flux qubit at its symmetry point. *Phys. Rev. Lett.* **105**, 060503 (2010).
54. Schoelkopf, R. J. & Girvin, S. M. Wiring up quantum systems. *Nature* **451**, 664 (2008).
55. Stern, M. *et al*. Flux qubits with long coherence times for hybrid quantum circuits. *Phys. Rev. Lett.* **113**, 123601 (2014).
56. Wilson, C. M. *et al*. Observation of the dynamical Casimir effect in a superconducting circuit. *Nature* **479**, 376 (2011).
57. Galiautdinov, A., Korotkov, A. N. & Martinis, J. M. Resonator–zero-qubit architecture for superconducting qubits. *Phys. Rev. A* **85**, 042321 (2012).

58. Ghosh, J. *et al*. High-fidelity controlled-σ z gate for resonator-based superconducting quantum computers. *Phys. Rev. A* **87**, 022309 (2013).
59. Stassi, R. *et al*. Quantum nonlinear optics without photons. *Phys. Rev. A* **96**, 023818 (2017).
60. Macrì, V., Nori, F. & Kockum, A. F. Simple preparation of Bell and GHZ states using ultrastrong-coupling circuit QED. *Phys. Rev. A* **98,** 062327 (2018).

Acknowledgements

This work was supported by National Natural Science Foundation of China under Grant Nos 61601196 and 61575055, the Foundation for Distinguished Young Scientists of Jiangxi Province Grant No. 20162BCB23009, Doctoral Foundation of University of Jinan Grant No. XBS1637.

Author Contributions

Xin Liu initiated the idea and carried out the critical calculations, Qinghong Liao and Guangyu Fang performed some calculations and contributed to the writing of manuscript. Shutian Liu guided the idea and examined the manuscript.

Additional Information

Competing Interests: The authors declare no competing interests.

Publisher's note: Springer Nature remains neutral with regard to jurisdictional claims in published maps and institutional affiliations.